Bull. Chem. Soc. Jpn. Vol. 80, No. 5, 960–962 (2007)

# Crystal Structure, Magnetic Properties, and Second Harmonic Generation of a Three-Dimensional Pyroelectric Cyano-Bridged Mn–Mo Complex

**Wataru Kosaka,[1,2] Tomohiro Nuida,[1,2] Kazuhito Hashimoto,[1] and Shin-ichi Ohkoshi*[1,2]**

[1]Department of Applied Chemistry, School of Engineering, The University of Tokyo, 7-3-1 Hongo, Bunkyo-ku, Tokyo 113-8656

[2]Department of Chemistry, School of Science, The University of Tokyo, 7-3-1 Hongo, Bunkyo-ku, Toyko 113-0033

Received October 23, 2006; E-mail: ohkoshi@chem.s.u-tokyo.ac.jp

A paramagnetic pyroelectric 3-dimensional cyano-bridged assembly, $[\{Mn^{II}(H_2O)_2\}\{Mn^{II}(pyrazine)(H_2O)_2\}\{Mo^{IV}(CN)_8\}]\cdot 4H_2O$ ($P2_1$) was synthesized. This compound displayed second harmonic generation with a value of $6.0 \times 10^{-11}$ esu.

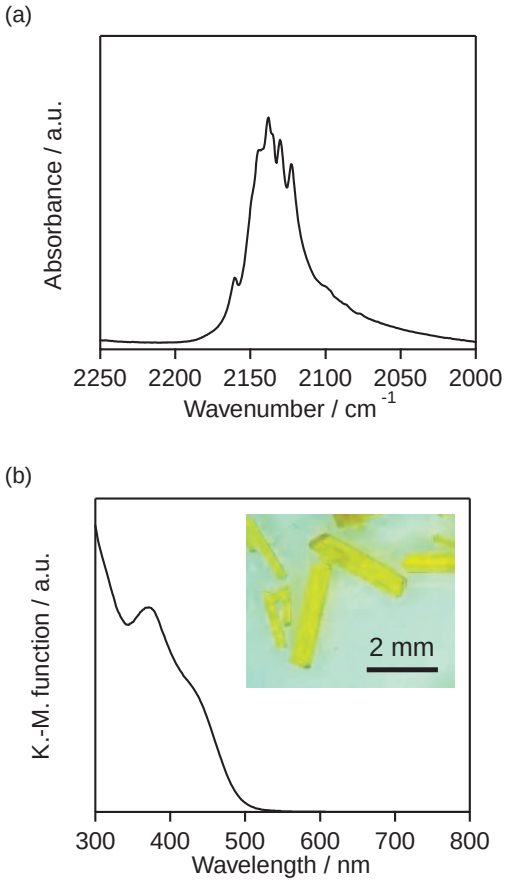


Fig. 1. (a) IR spectrum, (b) diffuse reflectance spectrum; inset, photograph of obtained crystals.

The magnetic properties of cyano-bridged metal assemblies have been extensively studied over the past decade due to their high Curie temperature and interesting functionalities.[1–3] Recently, octacyanometalate-based magnets have been aggressively studied. Octacyanometalates $[M(CN)_8]^{n-}$ (M = Mo, W, etc.) are a versatile class of building blocks that can adopt different spatial configurations, e.g., square antiprism ($D_{4h}$), dodecahedron ($D_{2d}$), bicapped trigonal prism ($C_{2v}$), depending on their chemical environment, such as the surrounding ligands. The materials of this series can take various coordination geometries in the crystal structure, that is, zero-dimensional (0-D),[4] 1-D,[5] 2-D,[6] and 3-D.[7] In this study, we prepared a novel 3-D pyroelectric Mn–Mo bimetal assembly, $[\{Mn^{II}(H_2O)_2\}\{Mn^{II}(pyrazine)(H_2O)_2\}\{Mo^{IV}(CN)_8\}]\cdot 4H_2O$. This compound showed second harmonic generation (SHG) due to its pyroelectric structure. In this paper, the crystal structure, magnetic properties, and SHG of this compound are described.

Yellow single crystals were obtained by slow diffusion of an aqueous solution of $K_4[Mo(CN)_8]$[8] (99.3 mg, 0.2 mmol) into an aqueous solution containing both $MnSO_4\cdot 5H_2O$ (96.4 mg, 0.4 mmol) and pyrazine (160.1 mg, 2 mmol). Yield: 57%. Elemental analyses by standard microanalytical methods confirmed that the formula of the compound was $[\{Mn^{II}(H_2O)_2\}\{Mn^{II}(pyrazine)(H_2O)_2\}\{Mo^{IV}(CN)_8\}]\cdot 4H_2O$. Anal. Calcd: C, 22.59; H, 3.16; N, 21.95%. Found: C, 22.31; H, 3.11; N, 21.89%.

In the IR spectra, CN stretching peaks due to bridging CN (2160, 2144, 2138, 2136, and 2130 $cm^{-1}$) and terminal CN (2123 $cm^{-1}$) were observed (Fig. 1a). In diffuse reflectance spectra, absorptions at 300, 370, and 430 nm (Fig. 1b) were observed. The absorption at 300 nm was assigned to charge transfer from $Mo^{IV}$ to $\pi^*$ orbital of cyano group, and the others were attributed to the d–d transition of $Mo^{IV}$.[9]

X-ray single crystal analysis showed that the crystal structure is monoclinic structure with a $P2_1$ space group ($a = 7.352(2)$ Å, $b = 14.131(5)$ Å, $c = 11.624(3)$ Å, $\beta = 98.72(2)^\circ$, $Z = 2$).[10] Figure 2 shows the asymmetric unit of the compound. The asymmetric unit consisted of $[Mo(CN)_8]^{4-}$, $[Mn1(H_2O)_2]^{2+}$, and $[Mn2(pyrazine)(H_2O)_2]^{2+}$. The coordination geometry around Mo and Mn sites were bicapped trigonal prism and pseudo-octahedron, respectively. Four of the CN groups in $[Mo(CN)_8]^{4-}$ were bridged to Mn1, and two of the CN groups were bridged to Mn2. The other two CN groups were free. Mo–C bond distances ranged from 2.139(2)–2.179(2) Å, and the Mo–C–N bonds were almost linear with angles between 175.5(2) and 179.0(2)°. Mn1 was coordinated by four cyanonitrogens at equatorial positions and two oxygen atoms of the water ligand at axial positions. The Mn1–N distances ranged from 2.186(2)–2.221(2) Å. Mn1–N–C bond angles ranged from 150.3(2)–176.6(2)°. Mn2 was coordinated by two nitrogen atoms of $[Mo(CN)_8]^{4-}$, two nitrogen atoms of pyrazine, and two oxygen atoms of the water ligand. The Mn2–$N_{CN}$ and Mn2–$N_{pyrazine}$ bond distances ranged from 2.142(2)–2.169(2) and 2.278(2)–2.283(2) Å, respectively.

Published on the web May 14, 2007; doi:10.1246/bcsj.80.960

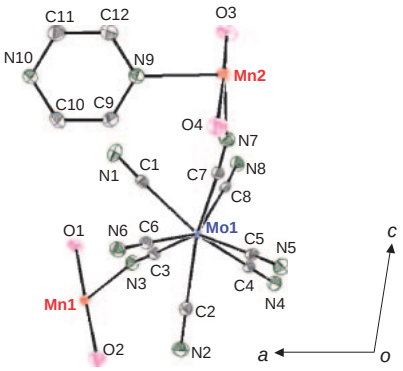


Fig. 2. ORTEP drawing of antisymmetric unit at 90 K with an atom numbering scheme. Displacement ellipsoids are drawn at a 50% probability level. Hydrogen atoms and non-coordinated water molecules are omitted for clarity.

Mn2–$N_{CN}$–$C_{CN}$ bond angles ranged from 163.6(2)–164.7(2)°. The cyano-bridged Mn1–Mo layer in the crystallographic *ab* plane (Fig. 3a) was linked by Mn2 through CN bridge in the crystallographic *c* direction (Fig. 3b), and Mn2 was also bridged by pyrazine in the *a* direction (Fig. 3c). Four water molecules existed between the layers as zeolitic waters. This compound is a pyroelectric material of a noncentrosymmetric space group ($P2_1$). The electric polarization is along *b* axis, since there is a 2-fold screw axis along this axis.

Figure 4 shows the magnetic susceptibility ($\chi_M$) under an applied field of 5000 G. The $\chi_M T$ value at 300 K was 8.7 K cm$^3$ mol$^{-1}$, which corresponds to the calculated spin-only moment value of 8.75 K cm$^3$ mol$^{-1}$ for $S_{Mn} = 5/2$ and $g_{Mn} = 2.00$. As the temperature decreased, the $\chi_M T$ value remained nearly constant until 20 K, and then, it decreased. Assuming the magnetic interaction between $Mn^{II}$ sites, the observed $\chi_M T$–$T$ plots were analyzed based on the molecular field approximation. In this approximation, $\chi_M = \chi_{Mn}/\{1-(2zJ/Ng^2\mu_B{}^2)\chi_{Mn}\}$, where $\chi_{Mn} = \Sigma S(S+1)(Ng^2\mu_B{}^2/3k_BT)$, $N$ is Avogadro number, $\mu_B$ is Bohr magneton, and $z$ is the number of the neighboring Mn atoms interacting with a Mn ion. The fitting parameters were $g = 2.0060(3)$ and $zJ = -6.89(5) \times 10^{-2}$ cm$^{-1}$ with $R = 1.7 \times 10^{-5}$ $(R = \Sigma[(\chi_M T)_{calcd} - (\chi_M T)_{obsd}]^2/\Sigma(\chi_M T)_{obsd}{}^2)$. The negative sign in the $J$ value suggests that the magnetic interactions between the $Mn^{II}$ via –NC–$Mo^{IV}$($S = 0$)–CN– bridge is weak antiferromagnetic coupling.

Since the $P2_1$ structure is a pyroelectric structure, SHG is expected in the present system. SHG measurements on a powder sample were conducted in the reflection mode (Fig. S1, Supporting Information). When the compound was irradiated by 1064 nm light by a Q-switched Nd:YAG laser at 294 K, 532 nm light was observed. Since the intensity of the 532 nm light increased with the square of the incident light intensity (Fig. 5), the observed 532 nm light is clearly SH light. The SHG susceptibility at the fundamental light of 1064 nm was $6 \times 10^{-11}$ esu. This value is 4% of the susceptibility for the famous SHG active crystal $KH_2PO_4$ (KDP).[11]

We prepared a paramagnetic pyroelectric 3-dimensional cyano-bridged Mn–Mo assembly. Since magnetic field-induced SHG is expected to be observed with this system, we will carry out the SHG measurement under magnetic field. In addition, when paramagnetic $[Nb(CN)_8]^{4-}$ is used in this assembly instead of diamagnetic $[Mo(CN)_8]^{4-}$, pyroelectric ferromagnet will be obtained. Since the observation of magnetization-induced SHG (MSHG)[3f,12] is expected, we are now preparing Mn–Nb system.

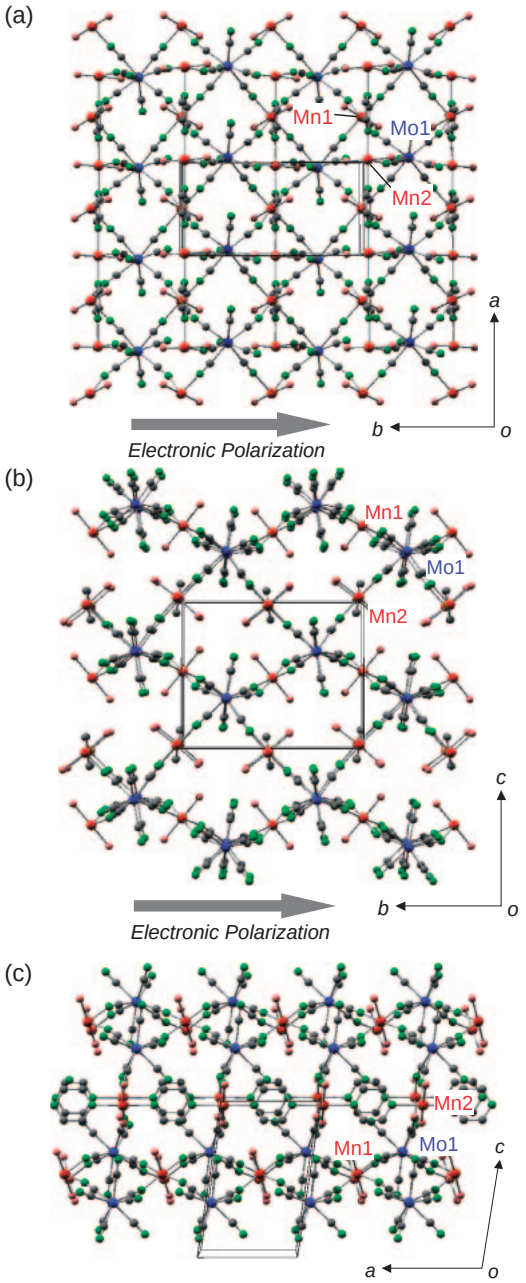


Fig. 3. Views of the crystal structure. Blue, red, gray, green, and pink balls represent Mo, Mn, C, N, and O, respectively. *P* represents electronic polarization. (a) The projection of 2-D layer in the *ab* plane. (b) The projection in the *bc* plane. (c) The projection in the *ac* plane.

Crystallographic data have been deposited with Cambridge Crystallographic Data Centre: Deposition number CCDC-628853. Copies of the data can be obtained free of charge via http://www.ccdc.cam.ac.uk/conts/retrieving.html (or from the Cambridge Crystallographic Data Centre, 12, Union Road, Cambridge, CB2 1EZ, UK; Fax: +44 1223 336033; e-mail: deposit@ccdc.cam.ac.uk).

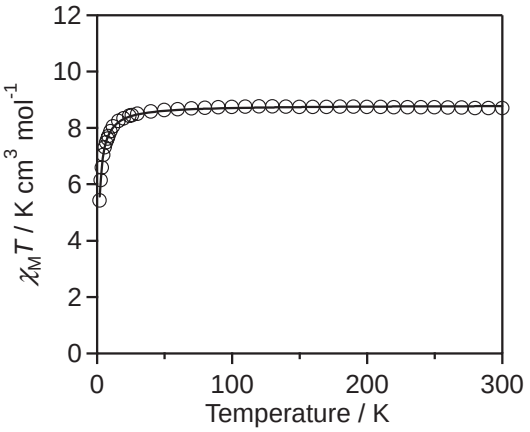


Fig. 4. Temperature dependence of $\chi_M T$–$T$ plots in an external magnetic field of 5000 G. The solid line represents the fitted line by the molecular field approximation.

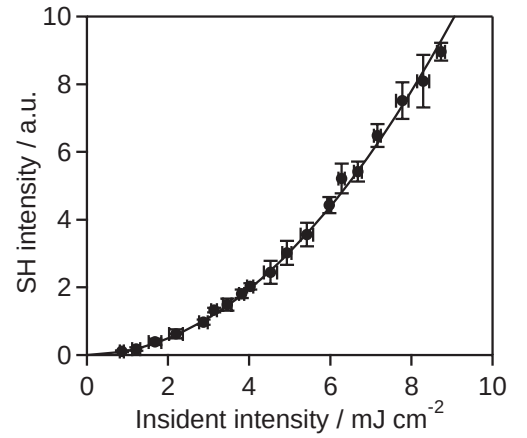


Fig. 5. SH intensity vs incident light intensity at 294 K (incident light: 1064 nm). The solid line represents the fitted curve using a quadratic function.

The present research is supported in part by a Grand-in-Aid for 21st Century COE Programs for Frontiers in Fundamental Chemistry and for Human-Friendly Materials based on Chemistry, a Grand-in-Aid for Scientific Research from the Ministry of Education, Culture, Sports, Science and Technology of Japan, and JSPS and RFBR under the Japan-Russia Research Cooperative Program.

## Supporting Information

Experimental details for the SHG measurements. This material is available free of charge on the web at: http://www.csj.jp/journals/bcsj/.

## References

1 a) M. Verdaguer, A. Bleuzen, C. Train, R. Garde, F. Fabrizi de Biani, C. Desplanches, *Philos. Trans. R. Soc. London, Ser. A* **1999**, *357*, 2959. b) J. S. Miller, *MRS Bull.* **2000**, *25*, 60. c) S. Ohkoshi, K. Hashimoto, *J. Photochem. Photobiol., C* **2001**, *2*, 71. d) K. R. Dunbar, R. A. Heintz, *Prog. Inorg. Chem.* **1997**, *45*, 283.

2 a) S. Ferlay, T. Mallah, R. Ouahès, P. Veillet, M. Verdaguer, *Nature* **1995**, *378*, 701. b) S. M. Holmes, G. S. Girolami, *J. Am. Chem. Soc.* **1999**, *121*, 5593. c) Ø. Hatlevik, W. E. Buschmann, J. Zhang, J. L. Manson, J. S. Miller, *Adv. Mater.* **1999**, *11*, 914. d) S. Ohkoshi, M. Mizuno, G. J. Hung, K. Hashimoto, *J. Phys. Chem. B* **2000**, *104*, 9365.

3 a) S. Ohkoshi, K. Arai, Y. Sato, K. Hashimoto, *Nat. Mater.* **2004**, *3*, 857. b) O. Sato, T. Iyoda, A. Fujishima, K. Hashimoto, *Science* **1996**, *272*, 704. c) S. Ohkoshi, Y. Abe, A. Fujishima, K. Hashimoto, *Phys. Rev. Lett.* **1999**, *82*, 1285. d) S. Margadonna, K. Prassides, A. N. Fitch, *J. Am. Chem. Soc.* **2004**, *126*, 15390. e) S. S. Kaye, J. R. Long, *J. Am. Chem. Soc.* **2005**, *127*, 6506. f) T. Nuida, T. Matsuda, H. Tokoro, S. Sakurai, K. Hashimoto, S. Ohkoshi, *J. Am. Chem. Soc.* **2005**, *127*, 11604. g) S. Ohkoshi, S. Ikeda, T. Hozumi, T. Kashiwagi, K. Hashimoto, *J. Am. Chem. Soc.* **2006**, *128*, 5320.

4 Z. J. Zhong, H. Seino, Y. Mizobe, M. Hidai, A. Fujishima, S. Ohkoshi, K. Hashimoto, *J. Am. Chem. Soc.* **2000**, *122*, 2952.

5 a) S. Ikeda, T. Hozumi, K. Hashimoto, S. Ohkoshi, *Dalton Trans.* **2005**, 2120. b) R. Podgajny, M. Balanda, M. Sikora, M. Borowiec, L. Spalek, C. Kapusta, B. Sieklucka, *Dalton Trans.* **2006**, 2801.

6 a) R. Podgajny, T. Korzeniak, M. Balanda, T. Wasiutynski, W. Errington, T. J. Kemp, N. W. Alcock, B. Sieklucka, *Chem. Commun.* **2002**, 1138. b) T. Hozumi, S. Ohkoshi, Y. Arimoto, H. Seino, Y. Mizobe, K. Hashimoto, *J. Phys. Chem. B* **2003**, *107*, 11571.

7 a) R. Garde, C. Desplanches, A. Bleuzen, P. Veillet, M. Verdaguer, *Mol. Crist. Liq. Cryst.* **1999**, *334*, 587. b) T. Kashiwagi, S. Ohkoshi, H. Seino, Y. Mizobe, K. Hashimoto, *J. Am. Chem. Soc.* **2004**, *126*, 5024. c) T. Hozumi, T. Nuida, K. Hashimoto, S. Ohkoshi, *Cryst. Growth Des.* **2006**, *6*, 1736.

8 J. G. Leipoldt, L. D. C. Bok, P. J. Cilliers, *Z. Anorg. Allg. Chem.* **1974**, *409*, 343.

9 a) J. R. Perumareddi, A. D. Liehr, A. W. Adamson, *J. Am. Chem. Soc.* **1963**, *85*, 249. b) H. Isci, W. R. Mason, *Inorg. Chim. Acta* **2004**, *357*, 4065.

10 Crystal data for $[\{Mn^{II}(H_2O)_2\}\{Mn^{II}(pyrazine)(H_2O)_2\}\{Mo^{IV}(CN)_8\}]\cdot 4H_2O$: $C_{12}H_{20}N_{10}O_8Mn_2Mo$, $M_r = 638.17$, monoclinic, space group $P2_1$, $a = 7.352(2)$, $b = 14.131(5)$, $c = 11.624(3)$ Å, $\beta = 98.72(2)^\circ$, $V = 1193.7(6)$ Å$^3$, $D_{calcd} = 1.78$ g cm$^{-3}$, $T = 90(1)$ K, $Z = 2$, $\mu$(Mo K$\alpha$) = 16.151 cm$^{-1}$, 5457 independent ($R_{int} = 0.020$) with 19312 observed data, $R1 = 0.031$, and $wR2 = 0.080$, goodness of fit: 1.010, Flack parameter: 0.18(2). A yellow single crystal having approximate dimension of $0.60 \times 0.30 \times 0.20$ mm$^3$ were mounted on a glass fiber. All measurements were made on a Rigaku RAXIS imaging plate area detector with graphite monochromated Mo K$\alpha$ radiation. The data were collected at a temperature of $90 \pm 1$ K. The structure was solved by direct methods using SIR97, expanded using Fourier techniques, and refined by full-matrix least-squares techniques by SHELXL-97. All non-hydrogen atoms were refined anisotropically. The hydrogen atoms of pyrazine and coordination water were refined using riding model. The hydrogen atoms of non-coordination water were not included during refinement. The absolute structure was deduced based on the Flack parameter. All calculations were performed using the Crystal Structure crystallographic software package.

11 R. J. Pressly, *CRC Handbook of Laser with Selected Data on Optical Technology*, The Chemical Rubber Co., Cleveland, **1971**.

12 S. Ohkoshi, J. Shimura, K. Ikeda, K. Hashimoto, *J. Opt. Soc. Am. B* **2005**, *22*, 196.